

Formation time dependence of femtoscopic $\pi\pi$ correlations in p+p collisions at $\sqrt{s_{NN}}=7$ TeV

Gunnar Gräf^{a,b}, Qingfeng Li^{a,c}, Marcus Bleicher^{a,b}

^aFrankfurt Institute for Advanced Studies, Frankfurt am Main, Germany

^bInstitut für Theoretische Physik, Goethe-Universität, Frankfurt am Main, Germany

^cSchool of Science, Huzhou Teachers College, Huzhou 313000, P.R. China

Abstract

We investigate femtoscopic $\pi\pi$ correlations using the UrQMD approach combined with a correlation afterburner. The dependence of $\pi\pi$ correlations on the charged particle multiplicity and formation time in p+p collisions at $\sqrt{s_{NN}}=7$ TeV is explored and compared to present ALICE data. The data allows to constrain the formation time in the string fragmentation to $\tau_f \leq 0.8$ fm/c.

1. Introduction

With the start of the LHC physics program two years ago a tremendous amount of new data became available. Apart from the heavy ion data, the proton-proton (pp) program allowed to explore collective features of the strong interaction in high multiplicity pp events.

It seems like in massive nucleus-nucleus collisions, a strongly interacting medium is created even in pp collisions, that exhibits similar bulk properties such as space momentum correlations and collective behaviour [1, 2, 3, 4]. The details of these correlations can be probed using Hanbury Brown-Twiss (HBT) [5] interferometry. While it is often argued, that the particle emitting system in p+p collisions is too small to create a medium that exhibits bulk properties, this is different at a center of mass energy of $\sqrt{s}=7$ TeV [6]. Here, the particle multiplicity is about the same as in nucleus-nucleus collisions, studied at the Relativistic Heavy Ion Collider (RHIC) in Brookhaven. For previous studies of femtoscopic correlations in p+p collisions at RHIC and Tevatron see [7, 8]. This data suggests that space momentum correlations are developed even in pp collisions as soon, as high particle multiplicities are

achieved. Thus, it is worthwhile studying the dependence of HBT observables on the event multiplicity. As the system created in p+p collisions at LHC is still small, an essential quantity that influences the particle freezeout radii is the formation time in flux tube fragmentation. Without going into the details of the specific implementation, it is clear that the formation time sets the scale for a minimum value of the source lifetime - of course followed by resonance decay and rescattering. In this paper we suggest, that the recent LHC data on pp collisions allows to determine the formation time in the flux tube break-up. Results for Pb+Pb reactions and scaling studies at the LHC within the same model can be found in [9, 10].

2. Two-particle correlations

To this aim we apply two-particle correlations to extract the space-time structure of ultra-relativistic particle collisions. For bosons the basic equation for the correlation function $C(\mathbf{q})$ is

$$C(\mathbf{q}, \mathbf{K}) = 1 + \frac{|\int d^4x S(x, K) e^{iq \cdot x}|^2}{|\int d^4x S(x, K)|^2}, \quad (1)$$

where $q = p_1 - p_2$, $K = \frac{1}{2}(p_1 + p_2)$, with p_1, p_2 being the four-momenta of the particles and $S(x, K)$ is the phase-space density of the particle emitting source. Using the Pratt-Bertsch parametrization we fit the resulting correlation function with the functional form

$$C(\mathbf{q}, \mathbf{K}) = 1 + \lambda(\mathbf{K}) \exp \left[- \sum_{i,j=o,s,l} q_i q_j R_{ij}^2(\mathbf{K}) \right], \quad (2)$$

using the *OSL*-system. Here, l is the longitudinal direction along the beam axis, o the out direction along the transverse component of \mathbf{K} and s the side direction perpendicular to the afore mentioned directions. $R_{ij}^2(\mathbf{K})$ are the HBT radii. All the radii in this paper are computed in the longitudinal comoving system (lcms).

The width of the pion pair separation in space is inversely proportional to the momentum difference q probing it. In the presence of flow, high p_\perp particles that are far apart in position space are very likely to be also far apart in momentum space. This results in smaller HBT radii than the actual

source size, because only the region of homogeneity is probed and not the entire source. For particles with low p_{\perp} the effect is not as strong, resulting in a larger probed region, thus giving larger HBT radii.

3. Particle formation time

The formation time denotes the time it takes for a hadron to be produced from a fragmenting string. A very common model to describe such a flux tube fragmentation is the Lund string model [11]. In the Lund model the formation time consists of the time it takes to produce a quark antiquark pair and the time it takes for that pair to form a hadron. For the Lund model both of these times are proportional to the transverse mass of the created hadron and inversely proportional to the string tension. For simplicity UrQMD uses a constant formation time of $\tau_f = 0.8 \text{ fm}/c$ for hard collisions. Only after the formation time particles, e.g. ρ -mesons, can decay or perform subsequent scatterings with their full cross section. During their formation time leading hadrons are allowed to interact with a reduced cross section. Other particles are not allowed to interact at all during their formation time. While a Heaviside function like behaviour of the cross section is implemented in UrQMD, there are other model studies [12, 13] that investigate the influence of several scenarios of continuous changes from zero to full cross section during the formation time. The freezeout space-time positions of hadrons are defined as either their point of formation or the point of last interaction, whatever occurs later in time. Since HBT probes the freezeout distribution the extracted radii are sensitive on the value of τ_f in small systems at high collision energies where the majority of particles is produced from flux tube fragmentation. Although there are many theoretical studies on the formation time [14, 15, 16, 17, 18] few of them allow to put constraints on τ_f or the behaviour of the cross section growth from experimental data.

4. Analysis process

The UrQMD (v3.3p1) is used to generate the freezeout distributions of particles in proton-proton collisions at $\sqrt{s_{NN}} = 7 \text{ TeV}$. For further information about UrQMD the reader is referred to [19, 20, 21]. After the simulation run, a correlation afterburner is applied to the freezeout distribution to calculate the corresponding 3D correlation function using Eq. 1. In this analysis, as in ALICE data, particles within a pseudorapidity interval of $|\eta| < 1.2$

$N_{charged}^{ \eta <1.2}$	UrQMD $\langle dN_{ch}/d\eta \rangle_{ \eta <1.2}$	ALICE $\langle dN_{ch}/d\eta \rangle_{ \eta <1.2}$
1-11	2.52	3.2
12-16	5.74	7.4
17-22	8.01	10.4
23-29	10.72	13.6
30-36	13.65	17.1
37-44	16.74	20.2
45-57	20.94	24.2
58-149	27.57	31.1

Table 1: Table of the investigated multiplicity intervals. The first column shows the interval boundaries, the second column the mean charged particle multiplicity per unit of pseudorapidity ($dN_{ch}/d\eta$) from events with at least one charged particle in $|\eta| < 1.2$ from UrQMD. The third column shows the same quantity from ALICE data [22].

are taken into account. The analysis is done differentially for K_{\perp} bins of 100 MeV in the region of $K_{\perp} = 0.1 - 1.0$ GeV and also for the different event multiplicities listed in Table 1. Generally the average $dN_{ch}/d\eta$ from UrQMD is 15% smaller than the one measured by the ALICE collaboration, in the same charged multiplicity classes, because we did not employ specific PYTHIA tunes for the present analysis. All the correlation functions are computed for pairs in the longitudinal comoving system (lcms). The HBT radii are extracted by fitting Eq. 2 to the 3-dimensional correlation functions over a range of $|q_i| < 800$ MeV.

5. Results

In this section the results on HBT radii from the UrQMD model are compared to ALICE data [22]. In Fig. 1 the projections in out, side and long direction of the 3D correlation function together with a projection of the fit for $K_{\perp}=0.3-0.4$ GeV and $N_{charged}^{|\eta|<1.2} = 23-29$ are shown as an example. It can be seen, that the calculated correlation function (shown as dots) is well described by a Gaussian fit (lines). However, oscillations of the correlation function are present at larger q . This indicates that there is a non-gaussian component in the underlying separation distribution of the pion freezeout points. Here we will not investigate this interesting question further.

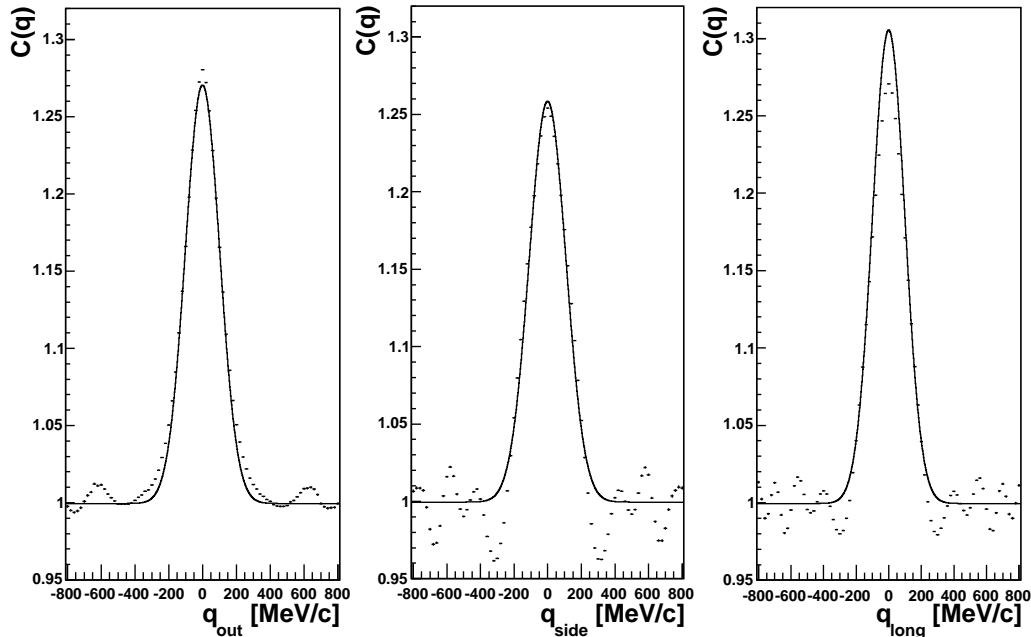


Figure 1: The dots represent projections of the 3 dimensional correlation function for $K_{\perp}=0.3-0.4$ GeV and $N_{charged}^{|\eta|<1.2} = 23-29$. The lines represent a χ^2 fit of Eq. 2 to the correlation function. Both the result of the fit and the correlation function are integrated over a range of $q_i = \pm 0.17$ GeV in the other directions for the purpose of projection.

The K_{\perp} dependence of the HBT radii extracted from the UrQMD freeze-out distribution is presented in Fig. 2 for the $dN_{ch}/d\eta$ classes defined in Tab. 1 in the pseudorapidity interval $|\eta| < 1.2$ in comparison to the ALICE data. The UrQMD calculations are presented for different values of the formation time τ_f ($\tau_f = 0.3$ fm/c, dashed lines; $\tau_f = 0.8$ fm/c, full lines; $\tau_f = 2$ fm/c, dotted lines). For $\tau_f = 0.3$ fm/c one obtains a good description for R_{out} , while R_{side} is slightly under predicted and the values for R_{long} are in line with data from ALICE. The choice $\tau_f = 0.8$ fm/c leads to a slight overestimation of R_{out} , however it leads to a reasonable description of R_{side} data. Also the K_{\perp} behaviour in R_{long} is much closer to the behaviour of the data. In contrast, a formation time of $\tau_f = 2$ fm/c, leads to a drastic over estimation of the data for all radii. Although there are discrepancies between model and data for all values of τ_f , the sensitivity on τ_f is much larger than those discrepancies. Therefore, the present ALICE data allows to constrain the formation time to values of $\tau_f \approx 0.3-0.8$ fm/c.

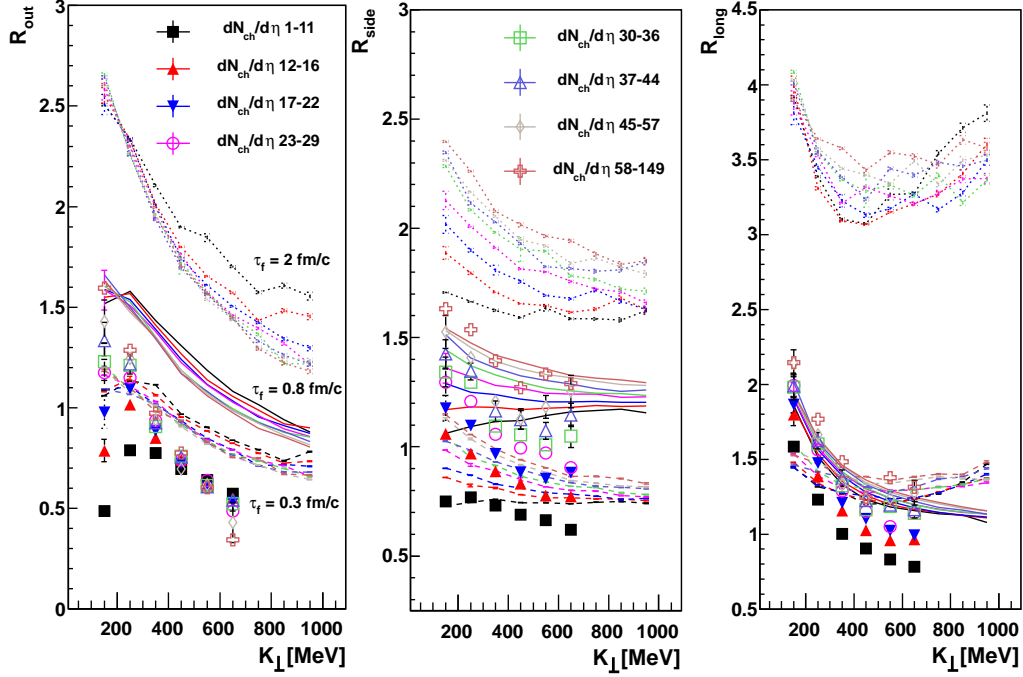


Figure 2: The lines represent HBT radii in pp collisions at $\sqrt{s}=7$ TeV from UrQMD for different multiplicities and formation times. The various line styles refer to results for $\tau_f = 0.3$ fm/c (dashed), $\tau_f = 0.8$ fm/c (default - full lines) and $\tau_f = 2$ fm/c (dotted). The colors represent the multiplicity classes as defined in table 1. The Points are data from the ALICE experiment [22].

Let us finally discuss the overall shape of the radii as a function of multiplicity and K_{\perp} . The R_{side} radii (see Fig. 2, middle) from UrQMD and in the data are flat as a function of K_{\perp} for low multiplicity events. With increasing multiplicity the radii develop a decrease towards higher K_{\perp} . This is exactly the behavior one would expect for the development of space-momentum correlations with rising event multiplicity [6]. For R_{out} (Fig. 2, left) however, there is a K_{\perp} dependence present in all multiplicity classes. Thus, only the development of radial flow with rising particle multiplicity seems not sufficient to explain the K_{\perp} dependence. Since R_{out} and R_{long} contain lifetime contributions of the source and R_{side} does not, there seems to be an additional non-trivial K_{\perp} and multiplicity dependence in the emission duration needed to explain the difference in the behaviour of R_{out} , R_{side} and R_{long} .

This additional correlation might be due to an additional momentum dependence in τ_f apart from the trivial Lorentz boost. This would lead to a direct effect on the emission duration, because it changes the particles production spacetime points. It would also lead to an indirect change of the emission region, since the particle rescattering is influenced by τ_f . In this case of pp collisions the effect of the rescattering should be negligible. Preformed hadron interactions become important in AA collisions [15, 23].

6. Summary

We have performed an analysis of proton-proton collisions at the top LHC energy of $\sqrt{s} = 7$ TeV. We have shown that the data provides rather direct access to the particle formation times in the flux tube fragmentation. The sensitivity to τ_f is large enough compared to the model uncertainties to find that a value $\tau_f = 0.3 - 0.8$ fm/c is strongly favored compared to larger values for τ_f . Values of $\tau_f \geq 2$ fm/c can be ruled out from the present analysis.

7. Acknowledgments

This work was supported by the Hessian LOEWE initiative through Helmholtz International Center for FAIR (HIC for FAIR). The Frankfurt Center for Scientific Computing (CSC) provided the computational resources. G.G. thanks the Helmholtz Research School for Quark Matter Studies (HQ-M) for support. Q.L. acknowledges the warm hospitality of FIAS institute and thanks the financial support by the key project of the Ministry of Education (No. 209053), the NNSF (Nos. 10905021, 10979023), the Zhejiang Provincial NSF (No. Y6090210), and the Qian-Jiang Talents Project of Zhejiang Province (No. 2010R10102) of China.

References

- [1] F. M. Liu and K. Werner, arXiv:1106.5909 [hep-ph].
- [2] F. M. Liu and K. Werner, Phys. Rev. Lett. **106** (2011) 242301 [arXiv:1102.1052 [hep-ph]].
- [3] S. Vogel, P. B. Gossiaux, K. Werner and J. Aichelin, Phys. Rev. Lett. **107**, 032302 (2011) [arXiv:1012.0764 [hep-ph]].

- [4] K. Werner, I. Karpenko, T. Pierog, M. Bleicher and K. Mikhailov, Phys. Rev. C **83**, 044915 (2011) [arXiv:1010.0400 [nucl-th]].
- [5] R. Hanbury Brown, R. Q. Twiss, Nature 27 (1956) 4497
- [6] K. Werner, K. Mikhailov, I. Karpenko and T. Pierog, arXiv:1104.2405 [hep-ph].
- [7] M. M. Aggarwal *et al.* [STAR Collaboration], arXiv:1004.0925 [nucl-ex].
- [8] T. Alexopoulos, C. Allen, E. W. Anderson, V. Balamurali, S. Banerjee, P. D. Beery, P. Bhat, J. M. Bishop *et al.*, Phys. Rev. **D48** (1993) 1931-1942.
- [9] Q. Li, G. Graef and M. Bleicher, arXiv:1203.4104 [nucl-th].
- [10] G. Graef, Q. Li and M. Bleicher, arXiv:1203.4071 [nucl-th].
- [11] B. Andersson, G. Gustafson, G. Ingelman, T. Sjostrand, Phys. Rept. **97**, 31-145 (1983).
- [12] C. Spieles *et al.*, Phys. Lett. B **458** (1999) 137.
- [13] K. Gallmeister and U. Mosel, Nucl. Phys. A **801**, 68 (2008) [nucl-th/0701064].
- [14] W. Cassing, K. Gallmeister and C. Greiner, Nucl. Phys. A **735**, 277 (2004) [hep-ph/0311358].
- [15] F. Arleo, Eur. Phys. J. C **30**, 213 (2003) [hep-ph/0306235].
- [16] B. Z. Kopeliovich, J. Nemchik and I. Schmidt, Nucl. Phys. A **782**, 224 (2007) [hep-ph/0608044].
- [17] T. Falter, W. Cassing, K. Gallmeister and U. Mosel, Phys. Rev. C **70**, 054609 (2004) [nucl-th/0406023].
- [18] A. Bialas, Phys. Lett. B **466**, 301 (1999) [hep-ph/9909417].
- [19] S. A. Bass *et al.*, Prog. Part. Nucl. Phys. **41** (1998) 255 [Prog. Part. Nucl. Phys. **41** (1998) 225] [arXiv:nucl-th/9803035].

- [20] H. Petersen, J. Steinheimer, G. Burau, M. Bleicher and H. Stoecker, Phys. Rev. C **78** (2008) 044901 [arXiv:0806.1695 [nucl-th]].
- [21] Q. Li, J. Steinheimer, H. Petersen, M. Bleicher, H. Stoecker, Phys. Lett. **B674** (2009) 111-116. [arXiv:0812.0375 [nucl-th]].
- [22] K. Aamodt *et al.* [ALICE Collaboration], [arXiv:1101.3665 [hep-ex]].
- [23] Q. Li, M. Bleicher and H. Stoecker, Phys. Lett. B **659**, 525 (2008) [arXiv:0709.1409 [nucl-th]].